

Recent results on a machine learning approach to event position reconstruction in the DEAP-3600 Dark Matter Search Experiment

Aidar Ilyasov* for the DEAP-3600 collaboration

*National Research Center “Kurchatov Institute”,
Kurchatov sq. 1, Moscow, Russia
National Research Nuclear University MEPhI,
Kashirskoe sh. 31, Moscow, Russia
E-mail: ilyasovaid@yandex.ru*

Machine learning is increasingly being applied in elementary particle physics, and the DEAP-3600 dark matter detector is no exception. One application of the new algorithm is the event position reconstruction in the detector. Here, we present updated results on the application of a fully-connected neural network for quality improvement. We also describe the structure of the neural network, its changes from the previous version, and a comparison with existing event position reconstruction algorithms.

****International Conference on Particle Physics and Cosmology****
*** 02-07, October 2023 ***
*** Yerevan, Armenia ***

*Speaker

1. Introduction

The Standard Model (SM) is the theory describing all known particle interactions. The discovery of the Higgs boson in 2012 completed the model. However, certain phenomena are still not accounted by the SM. Such problems, in particular, are the problem of neutrino oscillations and neutrino mass, as well as the problem of dark matter. Huge experiments are being conducted around the world to study these phenomena. Each of them has made progress, but we still don't know the origin and nature of dark matter (DM). Considering that, according to the latest result from the Planck experiment, DM makes up about 27 percent of the entire mass-energy of the Universe [1], discovering dark matter would bring key knowledge in the understanding the structure of the physical world. One of the detectors searching for dark matter is the DEAP-3600 detector.

2. The Detector

DEAP-3600 is a single-phase liquid argon (LAr) direct-detection dark matter experiment, operating 2 km underground at SNOLAB (Sudbury, Canada). The leading limit on the WIMP-nucleon spin-independent cross section on a LAr target of $3.9 \times 10^{-45} \text{ cm}^2$ ($1.5 \times 10^{-44} \text{ cm}^2$) for a 100 GeV/c² (1 TeV/c²) WIMP mass at 90% C. L. was reached during the last analysis [2]. The detector contains (3269 ± 24) kg LAr [3] during the second fill in a spherical acrylic vessel (AV) with an inner diameter of 1.7 m and viewed by 255 inward-facing 8" diameter Hamamatsu R5912 HQE low radioactivity photomultiplier tubes (PMTs), submerged in a water Cherenkov muon veto (MV) (Figure 1 (a)). The AV is coated on the inside with tetraphenyl butadiene (TPB) wavelength shifter [4], so that the LAr scintillation light, peaked at 128 nm, is converted to visible for efficient detection with PMTs surrounding the AV. The top 30 cm of the AV is filled with gaseous argon (GAr). The GAr/LAr interface is 55 cm above the equator of the AV. A full description of the detector can be found here elsewhere [5].

3. Motivation

One of the largest contribution to the background rate for the WIMP search is α particles. Signals from α -decays from short- and long-lived ²²²Rn progeny as well as short-lived ²²⁰Rn progeny are observed at several locations inside the detector [2].

These include the LAr target, the LAr/TPB and TPB/AV surfaces, and the surfaces of the acrylic flowguides (FGs) in the AV neck. After applying fiducial cuts, one of the largest contributions to the background rate is from ²¹⁰Po α -decays on the surfaces of the acrylic FGs in the AV neck (Figure 1 (b)). Scintillation light is observed from events in the neck, which are simulated with a thin LAr film coating the FGs. The FGs are not coated in TPB, and the acrylic absorbs most of the UV scintillation photons incident on their surfaces. This results in shadowed event topologies in which only a small fraction of the emitted photons reach the AV PMTs [2].

Despite the fact that fiducial cuts exclude most backgrounds, it greatly reduce the overall detector acceptance (Figure 2).

Therefore, there are two reasons to implement the new algorithm in analyzing the event position reconstruction in the detector:

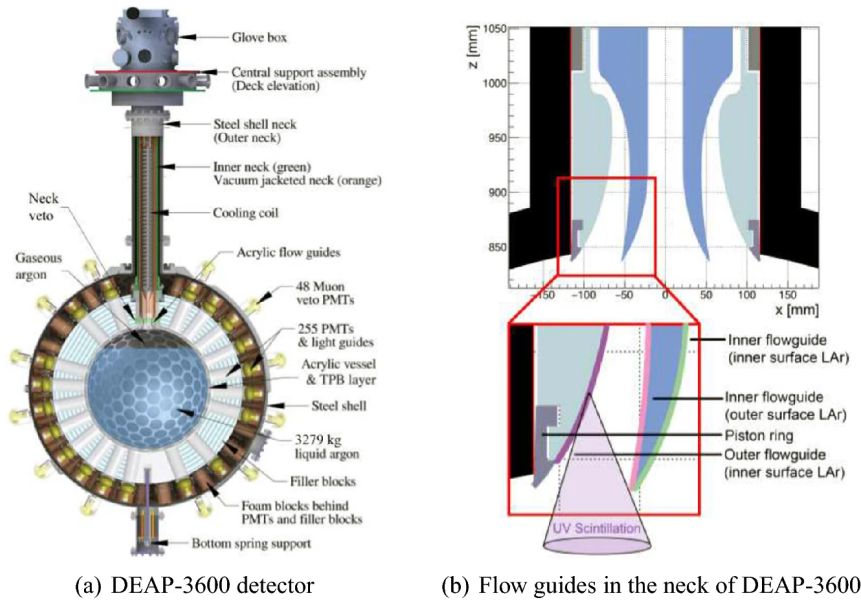


Figure 1: a: Schematic of the DEAP-3600 detector; b: Flowguide components in the AV neck [2]

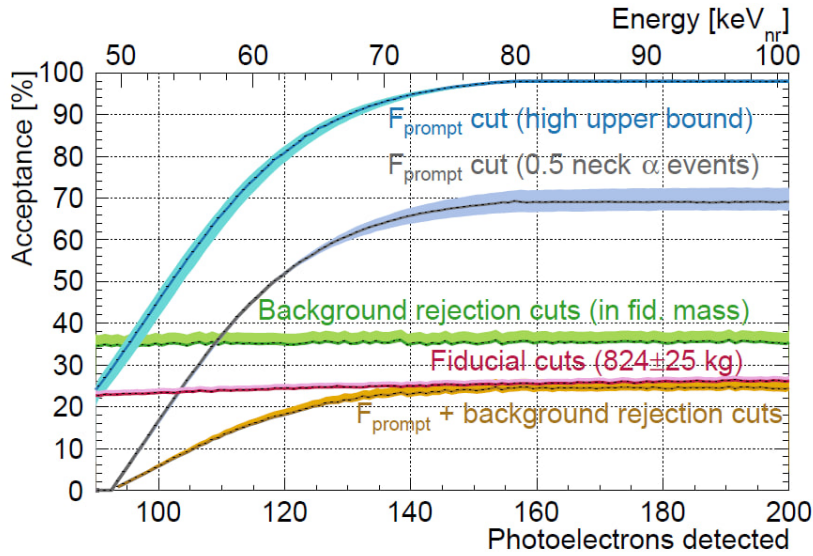


Figure 2: WIMP acceptance as a function of PE, broken down by cut type [2]

- To identify events occurred in the neck flowguides;
- To identify events in the bulk to increase the confidence radius and increase fiducial volume of the detector and its exposure.

Currently, two algorithms are used to reconstruct the event position in the detector. The first algorithm is called MBLikelihood (MBL) [2]. The main idea of the algorithm is simulating events in the LAr volume which is divided in a three-dimensional grid. The pattern of charges detected

by the 255 PMTs distributed around the LAr vessel is then used to build a likelihood function. A maximum likelihood procedure is then used for determining the event position.

The second algorithm is called TimeFit2 (TF2) [6]. This algorithm has a similar working principle, but it uses the time distribution of photon registration to make a pattern. The principle scheme of TimeFit2 position reconstruction algorithm is shown on Figure 3.

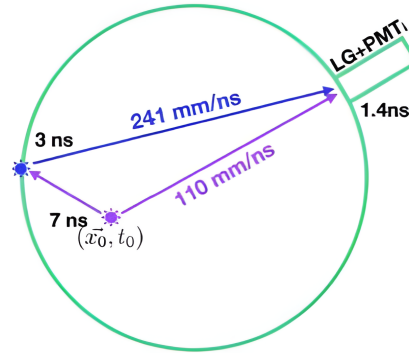


Figure 3: The principle scheme of TimeFit2 position reconstruction algorithm [6]

The likelihood functions in these algorithms operate under the assumption that events originate in the LAr bulk — this causes a bias in the case of events originating from the neck. Therefore, both algorithms work well in the LAr area of the detector, but for events in the neck region, they do not match in their results and cannot accurately determine the event position.

It was decided to use a neural network as a third algorithm to solve a set of problems to determine the position of such events.

4. Machine learning algorithm workflow

We are facing the following task: to create an algorithm that will work with good efficiency in the bulk volume but most importantly will be able to distinguish the events that occurred in the detector neck.

Different machine learning methods were tested and the most simple and effective resulted to be a neural network. [7–9]. The diagram of the neural network is shown in the Figure 4. It has the following main parts:

- A *neuron* is a mathematical function that calculates an output value by a weighted average of the sum of the incoming values. There are three types of neurons: input (into which the value of one of the variables from the training set is passed), output (from which the model prediction is taken) and hidden neurons (which are inside the model and in which intermediate computations take place). The type of mathematical function (activation function) in each neuron is the first main parameter for tuning the neural network.
- A *layer* is a set of neurons. The number of neurons in a layer and the number of hidden layers is the second main parameter for tuning the neural network. Only the number of input neurons (it is equal to the number of variables in the training set) and output neurons (it

is equal to the number of quantities to be determined) is fixed. By varying the number of neurons in hidden layers, as well as the number of hidden layers itself, the efficiency of the neural network can be controlled.

- Each neuron passes its value to the next layer with some *weight*:

$$y_i = F(X) = F\left(\sum w_i a_i\right),$$

where F is the activation function of the neuron, w_i is the weight of the connection which connects the current neuron with the i th neuron of the previous layer, and a_i is the output value of the i th neuron of the previous layer.

The main idea of neural network training is to tune these weight values. This parameter is the third and the most difficult to control during neural network tuning.

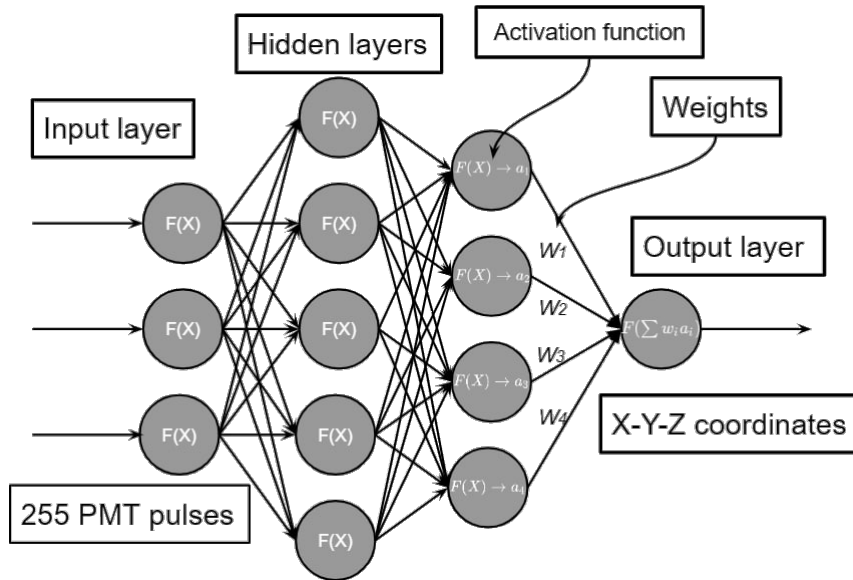


Figure 4: Schematic and operating principle of a fully connected neural network. a_i is the output value of the i th neuron of the previous layer [10]

For the current study, using the ROOT [11], Geant4 [12] and RAT [13] software packages, sets of Monte Carlo simulations of three types of events of 50,000 each were created: β -decays of ^{39}Ar , ^{40}Ar nuclear recoil events, and α -decays of ^{210}Po in the detector neck area (from all 3 flowguides in total). Therefore these 150,000 events were divided into training set (on which the model will be trained) and testing set (on which it will be tested with the blind analysis) at a ratio of 70:30. 255 values of charge detected at the internal PMTs, normalized on a scale from zero to one were used as input variables. As output variable we have X/Y/Z coordinate. It was decided to train the algorithm for all 3 coordinates separately to tune it more accurately.

The first result of this work can be found here [10]. This neural network structure worked well and detected neck events with high efficiency, but at the same time it often reconstructed events from the bulk volume above the real position.

After additional research, here we want to present an updated framework that performs better than the previous version.

As a result, the following neural network structure was used for X and Y coordinates (where in numerator/denominator we have the number of neurons and the activation function on each layer, respectively):

$$\frac{255 \text{ (Input)}}{\text{relu}} \rightarrow \frac{255}{\text{relu}} \rightarrow \frac{255}{\text{relu}} \rightarrow \frac{16}{\text{relu}} \rightarrow \frac{1 \text{ (Output)}}{\text{linear}}, \quad (1)$$

and a similar one for the Z coordinate:

$$\frac{255 \text{ (Input)}}{\text{relu}} \rightarrow \frac{1024}{\text{relu}} \rightarrow \frac{1024}{\text{relu}} \rightarrow \frac{1024}{\text{relu}} \rightarrow \frac{1 \text{ (Output)}}{\text{linear}}, \quad (2)$$

The main result of this structure is shown in Figure 5. We do not display the result for the Y coordinate as it is identical to the result for the X coordinate due to the symmetry of the detector.

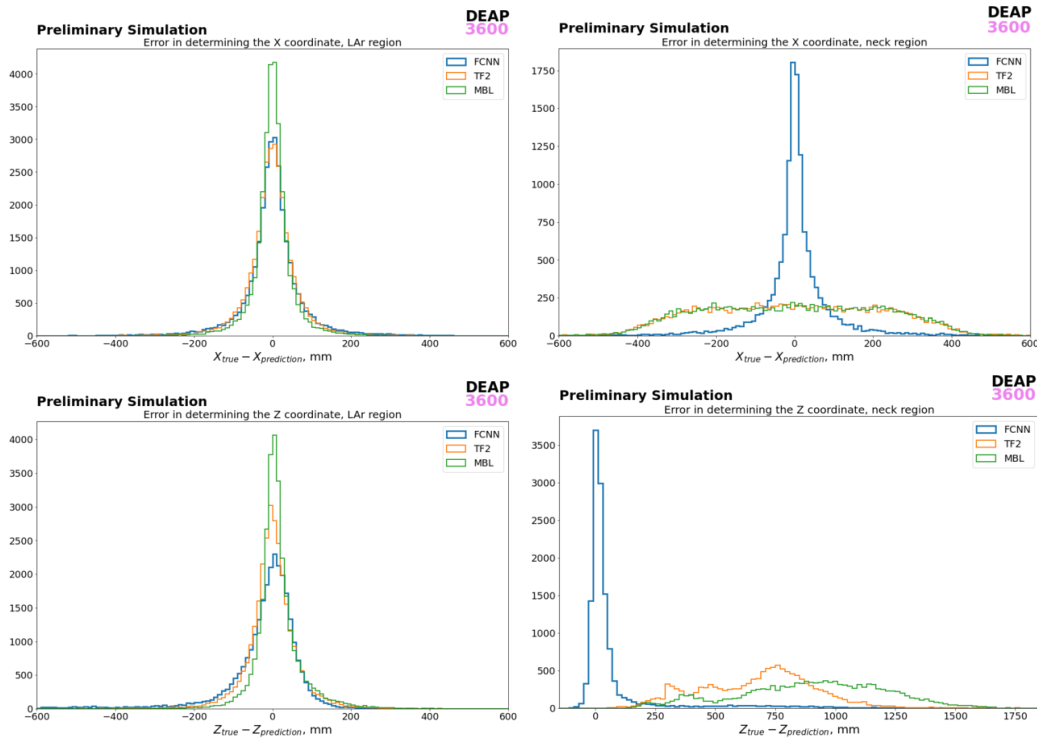


Figure 5: Errors of X (Y) and Z coordinate reconstruction for neural network (FCNN), MBlikelihood (MBL) and TimeFit2 (TF2). Left: Events originating from the LAr region. Right: Events originating from the neck region

Therefore, the present neural network model with a new structure works much better than the previous version. Now the events that actually occurred in the neck region are reconstructed less often in the bulk area, and the events that actually occurred in the bulk tend to be reconstructed less often in the neck region. This can be seen by the eliminated humps on both plots compared to the previous version of the algorithm [10].

5. Conclusion

Using Monte Carlo simulation, datasets totaling 150 thousand events were created for training and testing the neural network. After this, training procedures, setting up the neural network and testing it were carried out. Here, an improvement of the neural network model for detecting events in the neck of the DEAP-3600 detector was presented.

Acknowledgments

We thank the Natural Sciences and Engineering Research Council of Canada (NSERC), the Canada Foundation for Innovation (CFI), the Ontario Ministry of Research and Innovation (MRI), and Alberta Advanced Education and Technology (ASRIP), the University of Alberta, Carleton University, Queen's University, the Canada First Research Excellence Fund through the Arthur B. McDonald Canadian Astroparticle Physics Research Institute, Consejo Nacional de Ciencia y Tecnología Project No. CONACYT CB-2017-2018/A1-S-8960, DGAPA UNAM Grants No. PAPIIT IN108020 and IN105923, and Fundación Marcos Moshinsky, the European Research Council Project (ERC StG 279980), the UK Science and Technology Facilities Council (STFC) (ST/K002570/1 and ST/R002908/1), the Leverhulme Trust (ECF-20130496), the Russian Science Foundation (Grant No. 21-72-10065), the Spanish Ministry of Science and Innovation (PID2019-109374GB-I00) and the Community of Madrid (2018-T2/ TIC-10494), the International Research Agenda Programme AstroCeNT (MAB/2018/7) funded by the Foundation for Polish Science (FNP) from the European Regional Development Fund, and the European Union's Horizon 2020 research and innovation program under grant agreement No 952480 (DarkWave). Studentship support from the Rutherford Appleton Laboratory Particle Physics Division, STFC and SEPNet PhD is acknowledged. We thank SNOLAB and its staff for support through underground space, logistical, and technical services. SNOLAB operations are supported by the CFI and Province of Ontario MRI, with underground access provided by Vale at the Creighton mine site. We thank Vale for their continuing support, including the work of shipping the acrylic vessel underground. We gratefully acknowledge the support of the Digital Research Alliance of Canada, Calcul Québec, the Centre for Advanced Computing at Queen's University, and the Computational Centre for Particle and Astrophysics (C2PAP) at the Leibniz Supercomputer Centre (LRZ) for providing the computing resources required to undertake this work.

References

- [1] Planck Collaboration, *Planck 2018 results-vi. cosmological parameters*, *Astronomy & Astrophysics* **641** (2020) A6.
- [2] DEAP Collaboration, *Search for dark matter with a 231-day exposure of liquid argon using DEAP-3600 at SNOLAB*, *Physical Review D* **100** (2019) 022004.
- [3] DEAP Collaboration, *Precision measurement of the specific activity of ^{39}Ar in atmospheric argon with the DEAP-3600 detector*, *The European Physical Journal C* **83** (2023) 642.

- [4] DEAP Collaboration, *The liquid-argon scintillation pulse shape in deap-3600*, *The European Physical Journal C* **80** (2020) 1.
- [5] DEAP Collaboration, *Design and construction of the deap-3600 dark matter detector*, *Astroparticle Physics* **108** (2019) 1.
- [6] Y. Chen, *Position reconstruction using photon timing for the DEAP-3600 dark matter experiment*, *Journal of Instrumentation* **15** (2020) C05061.
- [7] F. Rosenblatt et al., *Principles of neurodynamics: Perceptrons and the theory of brain mechanisms*, vol. 55, Spartan books Washington, DC (1962).
- [8] R. Reed and R.J. MarksII, *Neural smithing: supervised learning in feedforward artificial neural networks*, MIT Press (1999).
- [9] J.J. Hopfield, *Neural networks and physical systems with emergent collective computational abilities.*, *Proceedings of the national academy of sciences* **79** (1982) 2554.
- [10] DEAP Collaboration, *Machine learning approach for event position reconstruction in the DEAP-3600 dark matter search experiment*, *MDPI Physics* **5** (2023) 483.
- [11] R. Brun and F. Rademakers, *ROOT—an object oriented data analysis framework*, *Nuclear Instruments and Methods in Physics Research Section A: Accelerators, Spectrometers, Detectors and Associated Equipment* **389** (1997) 81.
- [12] S. Agostinelli, J. Allison, K.a. Amako, J. Apostolakis, H. Araujo, P. Arce et al., *GEANT4—a simulation toolkit*, *Nuclear Instruments and Methods in Physics Research Section A: Accelerators, Spectrometers, Detectors and Associated Equipment* **506** (2003) 250.
- [13] T. Bolton, D. Gastler, J. Klein, H. Lippincott, A. Mastbaum, J. Nikkel et al., *RAT (is an analysis tool) user’s guide (2018)*, .